

# **Tropical low cloud feedback inferred from daily observations**

Robert Pincus,<sup>1,2</sup> K. Franklin Evans,<sup>3</sup> Dustin Swales<sup>1,2</sup>

---

Corresponding author: Robert Pincus, 325 Broadway R/PSD1, Boulder CO 80305, USA.  
(Robert.Pincus@colorado.edu)

<sup>1</sup>Cooperative Institute for Research in  
Environmental Sciences, University of  
Colorado, Boulder, Colorado, USA

<sup>2</sup>NOAA/Earth System Research Lab,  
Physical Sciences Division, Boulder,  
Colorado, USA

<sup>3</sup>Atmospheric and Oceanic Sciences,  
University of Colorado, Boulder, Colorado,  
USA

**Key Points.**

- Tropical low cloud feedback is estimated using observed relationships between albedo and environment
- Present-day relationships between albedo and environment imply positive feedbacks with warming

3 Varying responses of tropical low clouds to  
4 warming are at the heart of diversity in esti-  
5 mates of climate sensitivity obtained from mod-  
6 els. This study estimates the likely response  
7 independently, using observations of albedo  
8 and environmental conditions obtained from  
9 satellites and meteorological reanalysis on the  
10 daily time at which clouds respond to their  
11 environment. Statistical models are developed  
12 describing the relationships between albedo  
13 and the atmospheric conditions known to con-  
14 trol it. These relationships are applied to the  
15 change in those atmospheric conditions expected  
16 with surface warming, as inferred from climate  
17 model experiments. Observed relationships pre-  
18 dict dimmer tropical clouds with warming –

<sup>19</sup> a positive feedback on climate – at 2-4 times  
<sup>20</sup> the rate inferred from simulations alone.

## 1. Seeking observational constraints on low cloud climate feedbacks

Cloud feedbacks have been identified as one of the greatest sources of uncertainty in estimates of climate sensitivity since the very first assessments [*Charney et al.*, 1979]. Within the last decade it has become clear that tropical low clouds, in particular, are central to the differences in climate sensitivity in climate models [*Bony and Dufresne*, 2005]. The persistent diversity of model estimates of cloud feedbacks has inspired efforts to determine the magnitude and sign of the feedbacks from observations. Feedbacks determined from secular trends in surface temperature and cloud properties [*Eastman et al.*, 2011; *Seethala et al.*, 2015] remain highly uncertain due to the small signal of warming in the satellite epoch and the large observational uncertainties inherent in trying to measure small changes in cloud properties over time with ever-changing observing systems. Feedbacks might also be directly estimated from observations by assessing the sensitivity of cloud radiative effect to interannual variations in surface temperature either locally [*Eitzen et al.*, 2011; *Bellomo et al.*, 2014] or globally [e.g. *Dessler*, 2010; *Zhou et al.*, 2013], where global changes are driven primarily by the El Niño–Southern Oscillation. This approach assumes that environmental changes from small-amplitude short-term variations are consistent with those under long-term, larger amplitude climate change, as is supported by the behavior of climate models [*Zhai et al.*, 2015; *Zhou et al.*, 2015].

Observed relationships between clouds and their environment have also been used to inform model projections. One approach is to assume that models that more closely reproduce observed relationships are more likely to provide realistic projections of future behavior [e.g. *Clement et al.*, 2009; *Myers and Norris*, 2015] although model weighting,

including the rejection of models based on their ability to satisfy certain observational criteria, is not always well-justified [*Klocke et al.*, 2011; *Caldwell et al.*, 2014]. Alternatively, relationships observed in the past can be applied to future changes in environmental conditions as simulated by climate models [*Qu et al.*, 2014, 2015]. This exploits the larger environmental changes expected in a warmer world and provides a point of comparison for similar predictions from idealized [*Caldwell et al.*, 2013] or highly-detailed process models [*Bretherton et al.*, 2013; *Bretherton and Blossey*, 2014].

Progress to date has exploited variations in environmental parameters on time scales of a month or longer in order to reduce observational uncertainty. But the times scales on which clouds adjust to their environment are much shorter – typically hours for temperature and humidity within the cloud layer, and on the order of days for the depth of the combined boundary- and cloud layers [*Schubert et al.*, 1979; *Bellon and Stevens*, 2013; *Jones et al.*, 2014] – and relationships between clouds and their environment also change with time scale [c.f. *Klein and Hartmann*, 1993; *Klein*, 1997]. As one relevant example, the character of cloudiness is closely tied to subsidence at monthly time scales [*Bony and Dufresne*, 2005] but day-to-day variations are controlled far more strongly by the height and strength of the boundary layer inversion [*Brueck et al.*, 2015; *Nuijens et al.*, 2015], which reflects a balance between subsidence and surface forcing established over multi-day to weekly scales. Most efforts to determine the sensitivity of cloud properties to their environment have also been restricted to particular geographic regions, frequently those in which highly reflective marine stratocumulus are common, although low cloud feedbacks in climate models extend throughout the tropics [*Soden and Vecchi*, 2011].

Here we take a novel approach to estimating feedbacks from tropical low clouds stressing observations on time scales commensurate with those on which clouds are coupled to their environment and spanning the entire tropical ocean. We use satellite observations and meteorological reanalysis to build statistical models describing the dependence of low cloud albedo on environmental state on the short time scales at which clouds respond to their surroundings. Descriptions of environmental states in the present-day and in a future with uniform surface warmer are obtained from climate models. Our expectation is predictions of changes in atmospheric state by climate models are more robust than those of cloudiness or sea surface temperature, even if the present-day states may be in error. After correcting these states for errors in the representation of the present day we apply the statistical models to these states to estimate the distributions of low cloud albedo in the present and in the future. The difference between these albedos provides a feedback estimate consistent with observed present-day relationships between clouds and their environment.

## 2. Observed relationships between low cloud albedo and environmental conditions

To estimate cloud feedbacks from tropical oceanic low clouds we combine relationships between albedo and environmental state observed in the present day with estimates of how the distribution of states may change to infer the change in cloud albedo expected with warming. We focus on albedo itself because changes in reflection can be directly related to cloud feedbacks and to avoid quantitative difficulties in retrieving cloud fraction and cloud optical thickness [e.g. *Pincus et al.*, 2012], the two main controls on albedo,

where clouds sizes are commensurate with underlying sensor resolution. We neglect cloud impacts on terrestrial radiation entirely as these are quite small. Our domain encompasses all the tropical oceans equatorward of  $30^\circ$  latitude including much but not all of the stratocumulus regions.

## 2.1. Albedo and environmental state at daily timescales

Observations of low cloud albedo and estimates of the environmental state are obtained for the two-year period June 2009 to June 2011. Estimates of low cloud albedo are derived from Edition 2.6 of the Clouds and the Earth’s Radiant Energy System (CERES) SYN1DEG dataset [Doelling *et al.*, 2013]. CERES observations are available as day-time averages on a  $1^\circ$  latitude-longitude grid. Observations from Terra (morning) and Aqua (afternoon) platforms are averaged together. We exclude  $1^\circ$  regions in which aerosol optical depth at  $0.55\ \mu\text{m}$  is greater than 0.5, which comprise less than 1% of the tropical observations, and focus on low clouds (and cloud-free skies) by considering only those  $1^\circ$  regions in which mean cloud-top pressure exceeds 700 hPa. In the CERES SYN1DEG dataset high clouds cover about 43% of the  $1^\circ$  daily observations in the time two-year window we consider. Like the CERES Energy Balanced and Filled data [EBAF, Loeb *et al.*, 2009] SYN1DEG observations use observations from geostationary satellites to account for changes in cloud properties over the course of the day, but EBAF data are not available at daily time scales.

CERES converts measured broadband intensity to estimated hemispheric flux using empirical angular distribution models developed by accumulating observations of intensity made at different directions over time, controlling for the surface and fine-scale distri-

bution of cloud properties with each radiometer field of view [Loeb *et al.*, 2005]. The self-consistency of these angular distribution models [Loeb *et al.*, 2007] suggests that, for the oceanic low clouds with which we are concerned, the root-mean-square relative error in albedo is roughly 2.1% for overcast footprints of moderate optical depth and 4.7% for partly cloudy footprints of low optical depth. This error decreases with averaging so instantaneous estimates at 1 °scales are smaller than single footprint errors.

Tropospheric profiles of temperature, humidity, and wind at fixed pressure levels, estimates of surface temperature and latent and sensible heat fluxes, and integrated water vapor path come from the ERA-Interim reanalysis [Dee *et al.*, 2011]. From these we compute lower tropospheric (thermal) stability  $LTS \equiv \theta_{700} - \theta_{1000}$  [where  $\theta_p$  is the potential temperature at  $p$  hPa, Klein and Hartmann, 1993] and the rate of change of sea surface temperature following the local 1000 hPa wind  $SST_{adv} = \vec{u}_{1000} \cdot \nabla SST$ . Daily-averaged values are computed from the six-hourly fields provided by ERA-Interim.

Reanalysis fields in the tropics are more poorly constrained by observations than over mid-latitudes, especially in the lower troposphere where the microwave and infrared sounding instruments aboard satellites have little sensitivity. Our estimates of environmental conditions may therefore be somewhat biased by errors in the forecast model used to produce ERA-Interim, although we have focused on meteorological fields that are either well observed (and so well constrained in the reanalysis, e.g. sea surface temperature or free tropospheric humidity) or strongly constrained by atmospheric processes (e.g. near-surface temperature and humidity over the ocean).



The grids on which ERA-Interim and CERES data are available have the same  $1^\circ$  resolution but they are shifted by half a degree relative to one another, so we interpolate the ERA-Interim estimates of state to the CERES grid. Data volumes are reduced by sampling every ten days and by matching states to albedos only for the low-cloud scenes identified by CERES. The resulting data set contains roughly 155000 samples.

We also obtain the distribution of environmental conditions in the present-day and in idealized future climates by extracting daily-averaged fields from seven climate models (listed in Table 1) participating in the second phase of the Cloud Feedback Model Inter-comparison Project (CFMIP-2; see <http://cfmip.metoffice.com>), itself a component of fifth phase of the Coupled Model Intercomparison Project [CMIP5, see *Taylor et al.*, 2012]. Model-specific estimates of present-day climatology come from three years (1997-1999) of daily data from “AMIP” runs in which sea surface temperatures are specified. The time period differs from the period in which ERA-Interim and CERES observations were obtained because the AMIP experiments end in 2005. Conditions in the model amenable to high clouds are removed by eliminating columns in which the albedo of model-predicted mid- and high-clouds exceeds 1%. Mid- and high-cloud albedo is determined using the two-stream approximations applied to those elements of the joint distribution of optical thickness and cloud-top pressure reported by the “ISCCP simulator” [*Klein and Jakob*, 1999] with values of cloud-top pressure less than 700 hPa. Climate model fields are sampled in time to roughly match the sample size of the CERES/ERA-Interim data; the extent of this sampling depends on the spatial resolution and frequency of high clouds in each climate model. We determine albedo for the remaining columns as the ratio of

reflected to incident solar radiation at the top of the atmosphere. Estimates of idealized future conditions are obtained from “AMIP+4K” simulations in which sea surface temperature is uniformly increased by 4K. The seven models are all those for which the daily data we require (from the so-called ‘cfDay’ table) is available for both the AMIP and AMIP+4K experiments.

## 2.2. Describing relationships between albedo and environmental conditions

We build two classes of statistical models to describe relationships between daily-averaged low-cloud albedo and daily-averaged environmental conditions: one using multiple linear regression and another using nonlinear, non-parametric Bayesian neural networks following Chapter 10 of *Bishop* [1995]. The statistical models are trained on half the available data and tested against the other half to guard against fitting the model to random noise (over-fitting). We estimate model uncertainty using ten realizations, each trained on independent samples of half the available observations.

Statistical models can be built for arbitrary sets of environmental variables. We use an expansive state vector  $\mathbf{s}$  that includes essentially all environmental parameters thought to control boundary layer cloudiness [c.f. *Bretherton et al.*, 2013; *Myers and Norris*, 2015; *Qu et al.*, 2015]: sea surface temperature and its advective tendency following the 1000 hPa wind, pressure vertical velocity at 700 hPa, scalar wind speed at 1000 hPa, the specific humidity difference between these levels  $LTH \equiv q_{1000} - q_{700}$  and its thermodynamic analog LTS, described above, and the vertically-integrated water vapor path. The state vector also includes the cosine of the solar zenith angle at solar noon to account for the variation

in albedo with illumination angle. For illustrative purposes we also build a reduced state vector  $\hat{\mathbf{s}}$  that includes only solar zenith angle, LTS, and SST.

We build four statistical models (linear and nonlinear, using  $\mathbf{s}$  and  $\hat{\mathbf{s}}$ ) for the observations and for AMIP conditions in each of the climate models listed in Table 1. As might be expected, the richer state vector  $\mathbf{s}$  (filled symbols in Figure 1) is better able to fit albedo to environmental conditions than  $\hat{\mathbf{s}}$  (open symbols) regardless of the statistical model used, and nonlinear neural networks (circles) are better at fitting the relationships than is linear regression (squares). Here we assess skill using a close analogy to the  $R^2$  metric used in linear regression (1 minus the root-mean-square error in albedo predicted by the statistical model divided by the standard deviation of true albedo, evaluated against independent testing data and averaged over ten realizations). Observational uncertainty in both CERES estimates of albedo and ERA-Interim estimates of environmental parameters might be expected to make relationships noisier and less predictable, especially at daily times scales, than for the perfectly-known quantities from climate models, but in fact the models based on observations (shown in black) fit about as well as do models for some simulations, partly because low-cloud albedo is less variable in observations than in any of the climate models (colored symbols).

### 3. Future changes in tropical low cloud albedo

Low cloud feedbacks can be estimated by applying statistical models trained on present-day data to estimates of future conditions (here, taken from climate model AMIP+4K simulations described above) to determine albedo changes relative to present day. One danger is that statistical models, no matter how sophisticated, may not be accurate for

input data very different from the sample on which they are trained. Extrapolation to +4K conditions is not extreme relative to present-day variability (the standard deviation of SST in the ERA-Interim samples is 2.98K but it is possible that applying present-day albedo/environment relationships to these conditions will lead to errors in estimated albedo. We assess this risk using “perfect-model, perfect-observation” experiments, comparing the true change in mean low cloud albedo between present-day and +4K conditions in each climate model to the change predicted by statistical models trained on the climate model’s own present-day conditions (Figure 2). Here and below we report changes in mean low cloud albedo because this quantity controls feedback, but the mean is computed over roughly 155000 samples with ten realizations of each statistical model.

In all but one of the climate models low cloud albedo decreases in warmer climates, while extrapolation with statistical models predicts less dimming or even brightening. Neural networks have larger uncertainties when extrapolated than do regressions: the standard error of the prediction across ten realizations of all statistical models (colored lines) is relatively large for the neural networks and hardly visible for linear models. To the extent that Fig. 2 is indicative of general behavior it suggests that extrapolation to future conditions with statistical models will introduce errors in the sense of predicting overly bright low clouds in future.

The extrapolation in Fig. 2 includes only changes induced by 4K warming within each climate model. Applying statistical models based on observations to climate models states involves further extrapolation because the distribution of states in each climate model differs from the distribution of states obtained from ERA-Interim. We therefore

apply a correction to each climate model state vector  $\mathbf{s}_i^G$

$$\mathbf{s}'_i = \boldsymbol{\mu}^E + \mathbf{V}^E \sqrt{\frac{\lambda^E}{\lambda^G}} (\mathbf{V}^G)^\top (\mathbf{s}_i^G - \boldsymbol{\mu}^G) \quad (1)$$

where  $\boldsymbol{\mu}^E$  and  $\boldsymbol{\mu}^G$  are the mean state vectors and  $\lambda^E, \lambda^G, \mathbf{V}^E$  and  $\mathbf{V}^G$  the eigenvalues and eigenvectors, respectively, of the covariance matrix for present-day conditions in ERA-Interim and the climate model in question. We apply a similar correction to  $\hat{\mathbf{s}}_i$ . The correction ensures that the mean values and covariance matrix of the climate model's present-day distribution of states match those from ERA-Interim. (After correction the mean albedo of all climate models also matches the CERES estimate, which represents an independent check on the utility of the correction for the nonlinear models.) The same adjustment is applied to the distribution of AMIP+4K states.

We estimate the change in low cloud albedo with warming by applying statistical models describing observed relationships between albedo and environment to present-day and +4K conditions. The statistical models describe CERES low cloud albedo as a function of ERA-Interim environmental; a range of possible changes in future conditions is obtained from the adjusted distribution of state variables produced by each climate model under present-day and +4K conditions. Every estimate made with the extended set of variables  $\mathbf{s}$  indicates less reflective low clouds in warmer conditions (closed symbols along the abscissa of Figure 3) while estimates using only SST, LTS and cosine of the solar zenith angle ( $\hat{\mathbf{s}}$ ) on daily time scales indicate neutral or slightly brighter clouds, in contrast to the sensitivity inferred from observations on longer time scales [Qu *et al.*, 2014; Myers and Norris, 2015; Qu *et al.*, 2015].

As an attempt to isolate the contribution of large-scale circulation changes with warming the ordinate in Figure 3 shows the values of albedo change including all changes to environmental conditions except sea surface temperature. In models using  $\hat{\mathbf{s}}$  albedo is strongly sensitive to SST, whose change is specified across the models, explaining why the range of albedo change is quite small across different sets of future climate model environmental states. Models using the richer state vector  $\mathbf{s}$  show relatively little sensitivity to SST, however, because the true control on low cloud albedo is via dependencies on surface fluxes and boundary-layer humidity [Qu *et al.*, 2015]. Changes in albedo with warming are roughly consistent between the two classes of statistical models although the nonlinear neural networks are more uncertain as judged by the standard deviation across independent data samples (see also Fig. 2).

Predicted albedo change can be converted to climate feedback: the daytime mean insolation over our domain is  $763 \text{ W/m}^2$  so, to the extent that low clouds are uniformly distributed within the tropics, a 1% change in albedo for a 4 K temperature change indicates a daily-average low-cloud feedback of  $-0.954 \text{ W/m}^2 - \text{K}$ . Given this scaling linear regression provides a tropics-wide low-cloud feedback estimate of  $2.95 \pm 1.51 \text{ W/m}^2 - \text{K}$  and the nonlinear models  $2.66 \pm 1.16 \text{ W/m}^2 - \text{K}$  [comparable to the values from large-eddy simulation in Figure 5 of Bretherton, 2015], where the standard deviation accounts only for variations in future environmental conditions among climate models.

With one exception, present-day relationships between albedo and environmental conditions imply even greater reductions in tropical low cloud albedo than do the climate models used here (Figure 4). Most climate models in our set already produce low cloud

dimming with warming i.e. positive tropical low cloud feedbacks; taken on its face Fig. 4 rules out the possibility of negative feedback and implies that the strength of the feedback, which applies to roughly a quarter the planet's surface, is underestimated by the climate models by a factor of 2-4. Evidence from perfect-model, perfect-observation experiments (Fig. 2) suggests that predictions of cloud albedo by statistical models applied to warmer conditions are brighter than the true outcome, so that the more positive feedback inferred from observations may itself be an underestimate.

#### 4. Accumulating evidence for positive tropical cloud feedbacks

Our estimate of tropical low cloud feedback uses observations obtained over the entire tropical oceans at the time scales to which clouds respond to their environment (and on which process modeling is usually performed). Using daily observations also lets us exploit both the relatively short but high-quality observational record of flux from CERES as well as the relatively large co-variability in environmental state at short time scales. Because the change in environmental states is determined from surface warming in the absence of radiative forcing our estimates are restricted to temperature-dependent feedbacks while the changes realized in coming years will also include adjustments [Sherwood *et al.*, 2015] due to changes in CO<sub>2</sub> and other forcing agents. Applying a single set of observationally-based relationships between low cloud albedo and environmental state to future states estimated by climate models is consistent with the idea of correcting climate model sensitivities [Qu *et al.*, 2015] although it does not allow for feedbacks between clouds and atmospheric state.

Extrapolation with statistical models to future conditions in climate models underestimates the realized low cloud dimming with warming, implying that our positive estimates of tropical low cloud climate feedbacks may be biased towards smaller-than-realistic values. The sense of positive tropical low cloud climate feedbacks we infer, however, is consistent with a wide range of other approaches relying on observations at longer time scales [Clement *et al.*, 2009; Myers and Norris, 2015; Qu *et al.*, 2015, among others] and with insights from process-scale modeling [see Bretherton, 2015, for a thorough discussion] emphasizing increased vertical mixing with warming. Given observational evidence for positive high cloud feedbacks in the tropics [Xu *et al.*, 2007; Zelinka and Hartmann, 2011; Li *et al.*, 2012] the overall evidence for positive cloud feedbacks on climate is increasingly strong.

**Acknowledgments.** This work was supported by the National Science Foundation under award ATM-1138394. We appreciate helpful conversations with Louise Nuijens. This study used freely-available data: CERES data from <http://ceres.larc.nasa.gov/products.php?product=SYN>, ERA-Interim data from <http://data-portal.ecmwf.int>, and the CFMIP data from table cfDay for CMIP5 experiments AMIP and AMIP+4K from the Earth System Grid. We acknowledge the World Climate Research Programme's Working Group on Coupled Modelling, which is responsible for CMIP, and we thank the climate modeling groups listed in Table 1 for producing and making available their model output. For CMIP the U.S. Department of Energy's Program for Climate Model Diagnosis and Intercomparison provides coordinating support and led development of



software infrastructure in partnership with the Global Organization for Earth System  
Science Portals.

## References

- Bellomo, K., A. C. Clement, J. R. Norris, and B. J. Soden (2014), Observational and  
Model Estimates of Cloud Amount Feedback over the Indian and Pacific Oceans, *J.*  
*Climate*, *27*(2), 925–940.
- Bellon, G., and B. Stevens (2013), Time Scales of the Trade Wind Boundary Layer Ad-  
justment, *J. Atmos. Sci.*, *70*(4), 1071–1083.
- Bishop, C. M. (1995), *Neural Networks for Pattern Recognition*, Oxford University Press.
- Bony, S., and J.-L. Dufresne (2005), Marine boundary layer clouds at the heart of tropical  
cloud feedback uncertainties in climate models, *Geophys. Res. Lett.*, *32*(20).
- Bretherton, C. S. (2015), Insights into low-latitude cloud feedbacks from high-resolution  
models, *Phil. Trans. R. Soc. A*, *373*(2054), 20140,415.
- Bretherton, C. S., and P. N. Blossey (2014), Low cloud reduction in a greenhouse-warmed  
climate: Results from Lagrangian LES of a subtropical marine cloudiness transition, *J.*  
*Adv. Model. Earth Syst.*, *6*(1), 91–114.
- Bretherton, C. S., P. N. Blossey, and C. R. Jones (2013), Mechanisms of marine low cloud  
sensitivity to idealized climate perturbations: A single-LES exploration extending the  
CGILS cases, *J. Adv. Model. Earth Syst.*, *5*(2), 316–337.
- Brueck, M., L. Nuijens, and B. Stevens (2015), On the Seasonal and Synoptic Time-Scale  
Variability of the North Atlantic Trade Wind Region and Its Low-Level Clouds, *J.*  
*Atmos. Sci.*, *72*(4), 1428–1446.

- Caldwell, P. M., Y. Zhang, and S. A. Klein (2013), CMIP3 Subtropical Stratocumulus Cloud Feedback Interpreted through a Mixed-Layer Model, *J. Climate*, *26*(5), 1607–1625.
- Caldwell, P. M., C. S. Bretherton, M. D. Zelinka, S. A. Klein, B. D. Santer, and B. M. Sanderson (2014), Statistical significance of climate sensitivity predictors obtained by data mining, *Geophys. Res. Lett.*, *41*(5), 1803–1808.
- Charney, J. G., A. Arakawa, D. J. Baker, B. Bolin, R. E. Dickinson, R. M. Goody, C. E. Leith, H. M. Stommel, and C. I. Wunsch (1979), Carbon Dioxide and Climate: A Scientific Assessment, *Nat. Acad. Sci.*, p. 22.
- Clement, A. C., R. Burgman, and J. R. Norris (2009), Observational and Model Evidence for Positive Low-Level Cloud Feedback, *Science*, *325*(5939), 460–464.
- Dee, D. P., et al. (2011), The ERA-Interim reanalysis: configuration and performance of the data assimilation system, *Quart. J. Royal Met. Soc.*, *137*(656), 553–597.
- Dessler, A. (2010), A Determination of the Cloud Feedback from Climate Variations over the Past Decade, *Science*, *330*(6010), 1523–1527.
- Doelling, D. R., N. G. Loeb, D. F. Keyes, M. L. Nordeen, D. Morstad, C. Nguyen, B. A. Wielicki, D. F. Young, and M. Sun (2013), Geostationary Enhanced Temporal Interpolation for CERES Flux Products, *J. Atmos. Oceanic Technol.*, *30*(6), 1072–1090.
- Dufresne, J.-L., et al. (2013), Climate change projections using the IPSL-CM5 Earth System Model: from CMIP3 to CMIP5, *Climate Dyn.*, *40*(9-10), 2123–2165.
- Eastman, R., S. G. Warren, and C. J. Hahn (2011), Variations in Cloud Cover and Cloud Types over the Ocean from Surface Observations, 1954–2008, *J. Climate*, *24*(22), 5914–

5934.

Eitzen, Z. A., K.-M. Xu, and T. Wong (2011), An Estimate of Low Cloud Feedbacks from Variations of Cloud Radiative and Physical Properties with Sea Surface Temperature on Interannual Time Scales, *J. Climate*, *24*(4), 1106–1121.

Gent, P. R., et al. (2013), The Community Climate System Model Version 4, *J. Climate*, *24*(19), 4973–4991.

Jones, C. R., C. S. Bretherton, and P. N. Blossey (2014), Fast stratocumulus time scale in mixed layer model and large eddy simulation, *J. Adv. Model. Earth Syst.*, *6*(1), 206–222.

Klein, S. A. (1997), Synoptic Variability of Low-Cloud Properties and Meteorological Parameters in the Subtropical Trade Wind Boundary Layer, *J. Climate*, *10*(8), 2018–2039.

Klein, S. A., and D. L. Hartmann (1993), The Seasonal Cycle of Low Stratiform Clouds, *J. Climate*, *6*(8), 1587–1606.

Klein, S. A., and C. Jakob (1999), Validation and sensitivities of frontal clouds simulated by the ECMWF model, *Mon. Wea. Rev.*, *127*, 2514–2531.

Klocke, D., R. Pincus, and J. Quaas (2011), On constraining estimates of climate sensitivity with present-day observations through model weighting, *J. Climate*, *24*, 6092–6099.

Li, Y., P. Yang, G. R. North, and A. Dessler (2012), Test of the Fixed Anvil Temperature Hypothesis, *J. Atmos. Sci.*, *69*(7), 2317–2328.

Loeb, N. G., S. Kato, K. Loukachine, and N. Manalo-Smith (2005), Angular distribution models for top-of-atmosphere radiative flux estimation from the Clouds and the Earth’s Radiant Energy System instrument on the Terra satellite. Part I: Methodology, *J.*

*Atmos. Oceanic Technol.*, 22(4), 338–351.

Loeb, N. G., S. Kato, K. Loukachine, N. Manalo-Smith, and D. R. Doelling (2007), Angular distribution models for top-of-atmosphere radiative flux estimation from the Clouds and the Earth’s Radiant Energy System instrument on the Terra satellite. Part II: Validation, *J. Atmos. Oceanic Technol.*, 24(4), 564–584.

Loeb, N. G., B. A. Wielicki, D. R. Doelling, S. Kato, T. Wong, G. L. Smith, D. F. Keyes, and N. Manalo-Smith (2009), Toward Optimal Closure of the Earth’s Top-of-Atmosphere Radiation Budget, *J. Climate*, 22(3), 748–766.

Myers, T. A., and J. R. Norris (2015), On the Relationships between Subtropical Clouds and Meteorology in Observations and CMIP3 and CMIP5 Models, *J. Climate*, 28(8), 2945–2967.

Nuijens, L., B. Medeiros, I. Sandu, and M. Ahlgrimm (2015), Observed and modeled patterns of covariability between low-level cloudiness and the structure of the trade wind layer, *J. Adv. Model. Earth Syst.*, 7, 1741–1764.

Pincus, R., S. Platnick, S. A. Ackerman, R. S. Hemler, and R. J. P. Hofmann (2012), Reconciling simulated and observed views of clouds: MODIS, ISCCP, and the limits of instrument simulators, *J. Climate*, 25, 4699–4720.

Qu, X., A. Hall, S. Klein, and P. Caldwell (2014), On the spread of changes in marine low cloud cover in climate model simulations of the 21st century, *Climate Dyn.*, 42(9-10), 2603–2626.

Qu, X., A. Hall, S. A. Klein, and A. M. DeAngelis (2015), Positive tropical marine low-cloud cover feedback inferred from cloud-controlling factors, *Geophys. Res. Lett.*, 42(18),

7767–7775.

Schubert, W. H., J. S. Wakefield, E. J. Steiner, and S. K. Cox (1979), Marine Stratocumulus Convection. part II: Horizontally Inhomogeneous Solutions, *J. Atmos. Sci.*, *36*(7), 1308–1324.

Seethala, C., J. R. Norris, and T. A. Myers (2015), How Has Subtropical Stratocumulus and Associated Meteorology Changed since the 1980s?, *J. Climate*, *28*(21), 8396–8410.

Sherwood, S. C., S. Bony, O. Boucher, C. Bretherton, P. M. Forster, J. M. Gregory, and B. Stevens (2015), Adjustments in the forcing-feedback framework for understanding climate change, *Bull. Amer. Meteor. Soc.*, *96*, 217–228.

Soden, B. J., and G. A. Vecchi (2011), The vertical distribution of cloud feedback in coupled ocean-atmosphere models, *Geophys. Res. Lett.*, *38*(12), L12,704.

Stevens, B., et al. (2013), Atmospheric component of the MPI-M Earth System Model: ECHAM6, *J. Adv. Model. Earth Syst.*, *5*(2), 146–172.

Taylor, K. E., R. J. Stouffer, and G. A. Meehl (2012), An Overview of CMIP5 and the Experiment Design, *Bull. Amer. Meteor. Soc.*, *93*(4), 485–498.

The HadGEM2 Development Team G M Martin, et al. (2011), The HadGEM2 family of Met Office Unified Model climate configurations, *Geoscientific Model Development*, *4*(3), 723–757.

von Salzen, K., et al. (2013), The Canadian Fourth Generation Atmospheric Global Climate Model (CanAM4). Part I: Representation of Physical Processes, *Atmos.-Ocean*, *51*(1), 104–125.

Watanabe, S., et al. (2011), MIROC-ESM: model description and basic results of CMIP5-20c3m experiments, *Geoscientific Model Development*, 4(2), 1063–1128.

Xu, K.-M., T. Wong, B. A. Wielicki, L. Parker, B. Lin, Z. A. Eitzen, and M. Branson (2007), Statistical Analyses of Satellite Cloud Object Data from CERES. Part II: Tropical Convective Cloud Objects during 1998 El Niño and Evidence for Supporting the Fixed Anvil Temperature Hypothesis, *J. Climate*, 20(5), 819–842.

Yukimoto, S., et al. (2012), A New Global Climate Model of the Meteorological Research Institute: MRI-CGCM3 - Model Description and Basic Performance, *Journal of the Meteorological Society of Japan. Ser. II*, 90A IS -, 23–64.

Zelinka, M. D., and D. L. Hartmann (2011), The observed sensitivity of high clouds to mean surface temperature anomalies in the tropics, *J. Geophys. Res.*, 116(D23), D23103.

Zhai, C., J. H. Jiang, and H. Su (2015), Long-term cloud change imprinted in seasonal cloud variation: More evidence of high climate sensitivity, *Geophys. Res. Lett.*, 42(20), 8729–8737.

Zhou, C., M. D. Zelinka, A. E. Dessler, and P. Yang (2013), An Analysis of the Short-Term Cloud Feedback Using MODIS Data, *J. Climate*, 26(13), 4803–4815.

Zhou, C., M. D. Zelinka, A. E. Dessler, and S. A. Klein (2015), The relationship between interannual and long-term cloud feedbacks, *Geophys. Res. Lett.*, 42(23), 10,463–10,469.

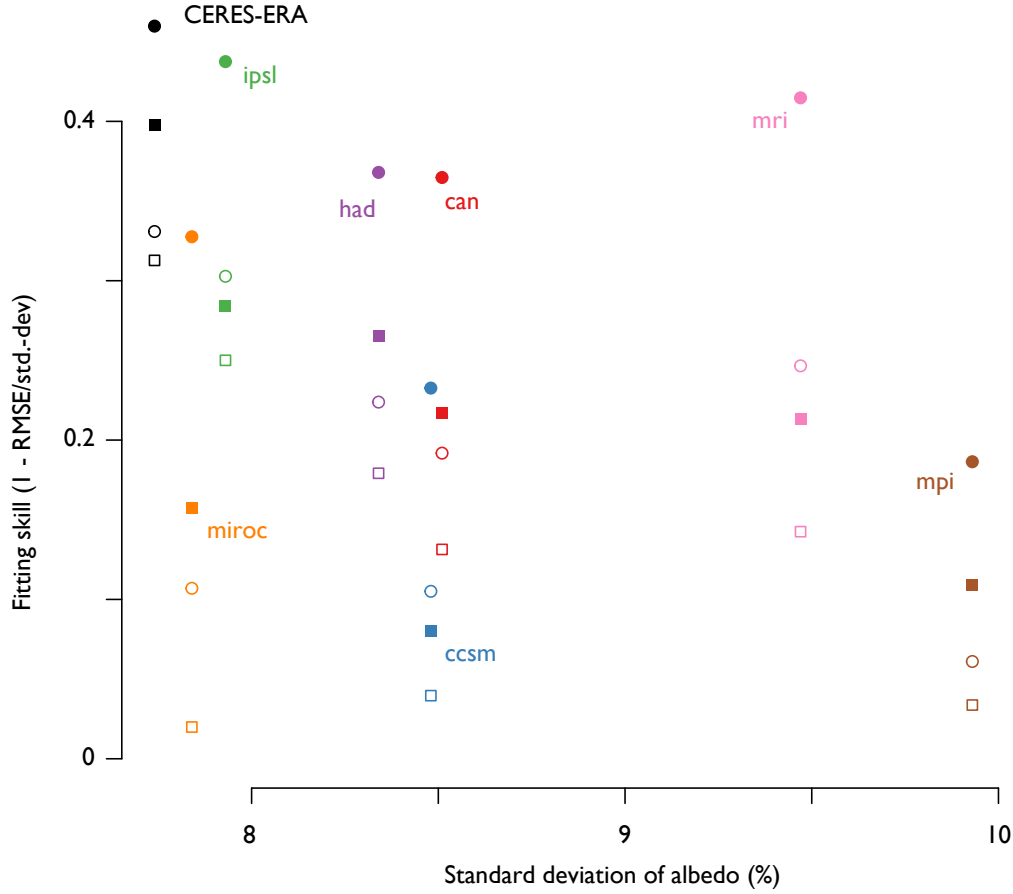


**Figure 1.** Skill in statistical models fitting low cloud albedo to environmental conditions at daily time scales. Nonlinear, non-parametric models (circles) are better able to fit albedo to environmental conditions than is multiple linear regression (squares) and a richer set of predictors (closed symbols) leads to better fits and lower error than a reduced set (open symbols). Skill is measured against independent testing data as 1 minus the root-mean-square error divided by the standard deviation of albedo. Low-cloud albedo measured by CERES (black) is somewhat less variable, and somewhat easier to fit to environmental conditions, than is albedo from most available climate models (colors).

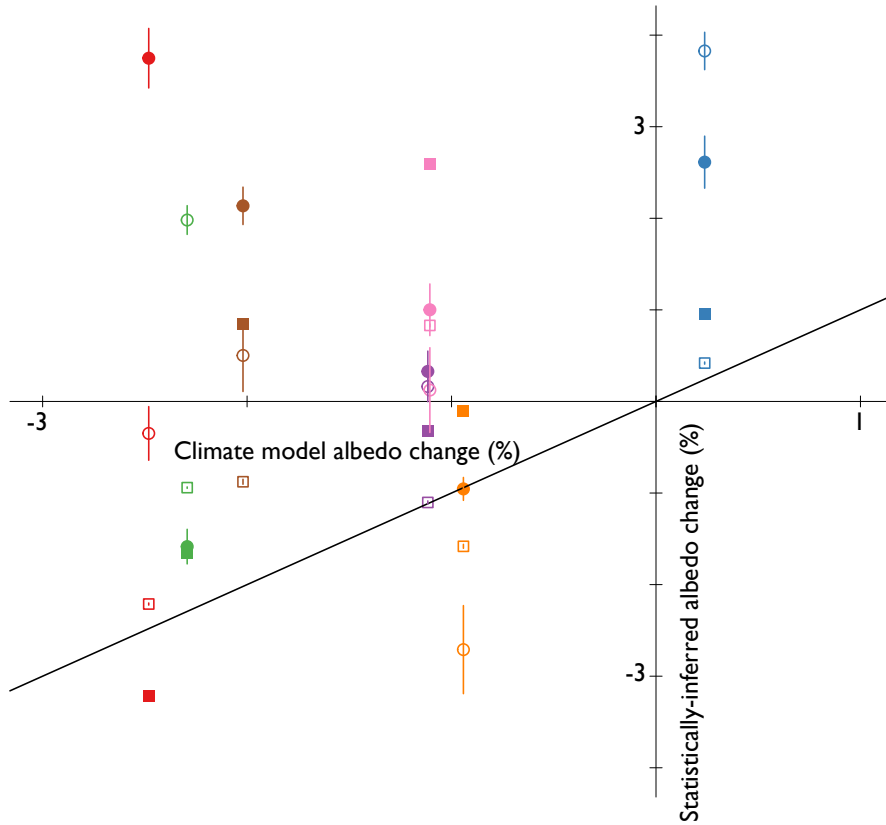


**Figure 2.** Change in low-cloud albedo (%) in seven climate models between +4K and present-day conditions predicted by statistical models as a function of the true warming. The diagonal line indicates equality. The statistical models are trained on albedo and environmental conditions for each climate model (distinguished using the same color scheme as in Fig. 1) separately. Nonlinear models extrapolate less well to future conditions and hence are substantially more uncertain as indicated by the standard deviation among ten independent realizations (vertical bars). Essentially all climate models produce less reflective low clouds in warmer conditions; statistical models either underestimate the amount of dimming or predict more reflective low clouds.



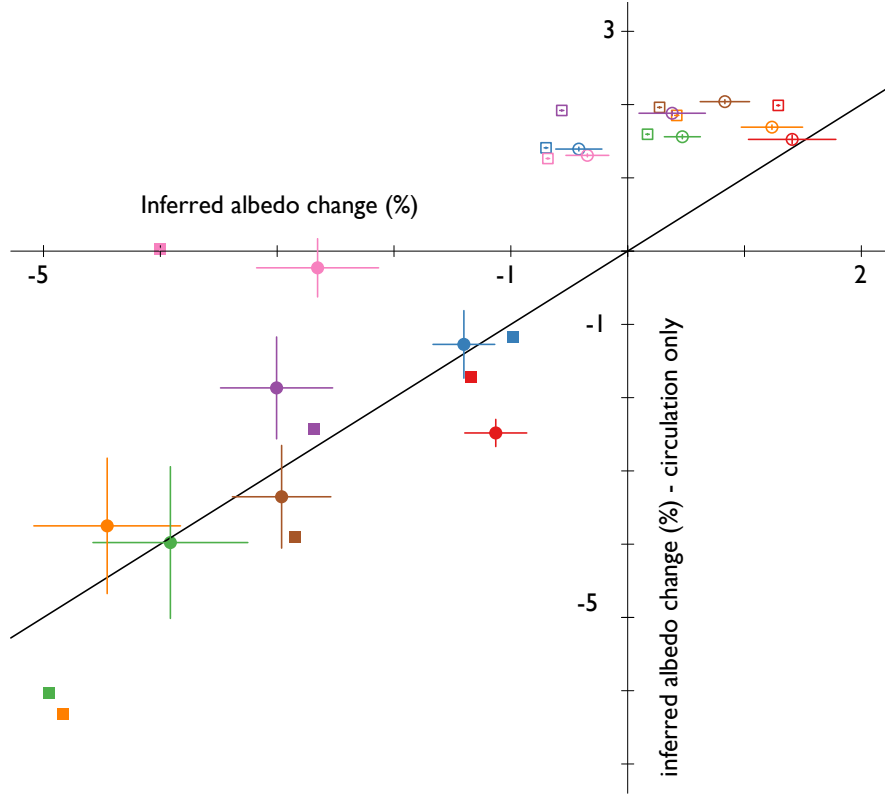


**Figure 3.** Change in low-cloud albedo (%) predicted by applying statistical models trained on present-day observations to changes in the distribution of environmental states predicted by climate models when sea surface temperature is raised uniformly by 4 K. Values on the abscissa show the albedo change associated with warmer conditions; values on the ordinate show the change due to “circulation” diagnosed by suppressing the sea surface change. Each percentage change in albedo corresponds to a low cloud feedback of  $0.954 \text{ W/m}^2 - \text{K}$ . The diagonal line indicates equality.

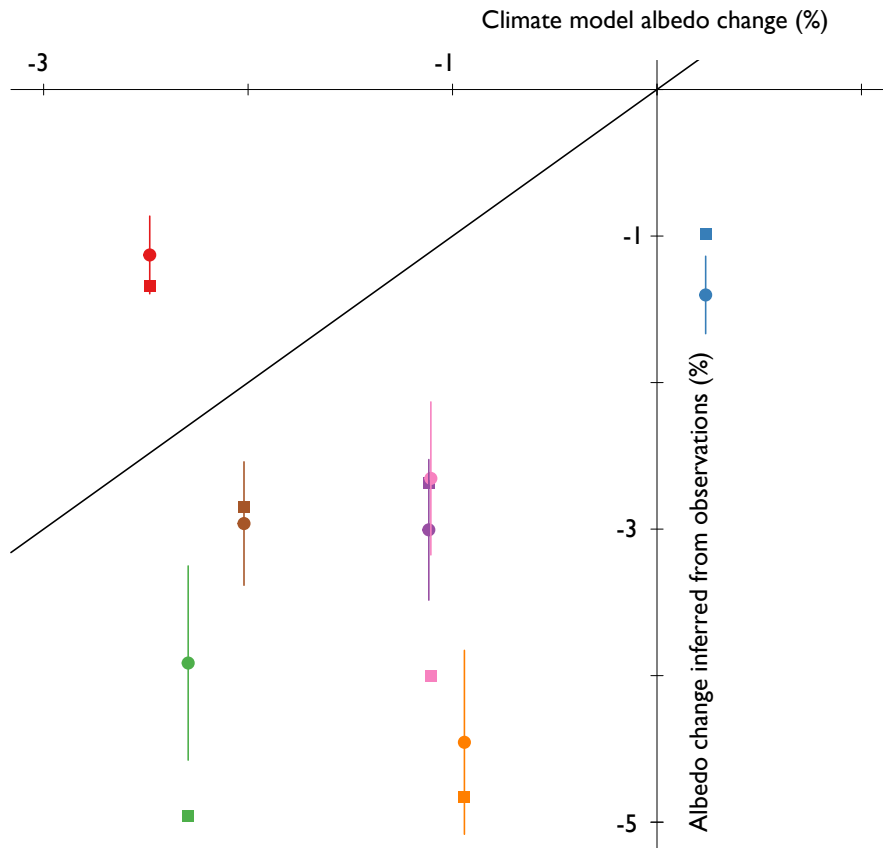


**Figure 4.** Change in low-cloud albedo (%) predicted by statistical models as a function of the albedo change predicted by the climate models themselves. The diagonal line indicates equality. Although most climate models predict less reflective low clouds in warmer conditions, observed relationships between albedo and environmental state suggest that this dimming is under-predicted, while perfect model results in Fig. 2 suggest that even the statistical predictions of future low cloud albedo are too bright.

**Table 1.** Atmospheric models used to estimate future changes in environmental conditions

CMIP5 model name	Institution	Reference
Can-AM4	Canadian Centre Climate Modeling and Analysis	<i>von Salzen et al.</i> [2013]
CCSM4	National Center for Atmospheric Research	<i>Gent et al.</i> [2013]
Had-GEM2-A	UK Met. Office	<i>The HadGEM2 Development Team</i>
IPSL-CM5A-LR	Institut Pierre Simon Laplace	<i>Dufresne et al.</i> [2013]
MIROC	Atmosphere and Ocean Research Institute	<i>Watanabe et al.</i> [2011]
MPI-ESM-LR	Max Planck Institute for Meteorology	<i>Stevens et al.</i> [2013]
MRI-CGCM3	Meteorological Research Institute	<i>Yukiomoto et al.</i> [2012]